Journal of Alloys and Compounds 488 (2009) 89–99

Contents lists available at ScienceDirect

Journal of Alloys and Compounds

journal homepage: www.elsevier.com/locate/jallcom

Study of the influence of copper and magnesium additions on the microstructure formation of Zn–Al hypoeutectic alloys

Eleani M. da Costa[a], Cesar Edil da Costa[b], Felipe Dalla Vecchia[a], Cristiane Rick[a], Maurício Scherer[a], Carlos A. dos Santos[a,*], Berenice A. Dedavid[a]

[a] *Pontifical Catholic University of Rio Grande do Sul, Faculty of Engineering and Post-Graduation Program in Materials Engineering and Technology, Av. Ipiranga, 6681, Prédio 30, CEP 90.619-900, Porto Alegre, RS, Brazil*
[b] *State University of Santa Catarina, Department of Mechanical Engineering, Bairro Bom Retiro, CEP 89.223-100, Joinville, SC, Brazil*

ARTICLE INFO

Article history:
Received 29 June 2009
Received in revised form 22 August 2009
Accepted 25 August 2009
Available online 31 August 2009

Keywords:
Zn–Al hypoeutectic alloys
Computer-Aided Cooling Curve Analysis
Microstructure formation
Solidification
Hardness
Phase transformation

ABSTRACT

In this paper the influence of copper and magnesium content in the microstructural evolution during the solidification of Zn–4 wt.% Al hypoeutectic alloys was investigated using the CA-CCA method (Computer-Aided Cooling Curve Analysis) and SEM (Scanning Electron Microscopy). The identification of chemical composition of the phases and microconstituents was done by SEM using the EDS (Energy Dispersive X-Ray Spectroscopy) operation mode. For that purpose, ternary and quaternary alloys were prepared with different amounts of copper and magnesium. The influence of both copper and magnesium amounts on the transformation temperatures of the Zn–Al based hypoeutectic alloys was evident in the distinct microstructures formed during solidification as well as in the cooling curves obtained by thermal analyses, promoting modifications in solid–liquid temperature range, in the kinetic and also in the chemical compositions of the phase transformation. The addition of extra copper promoted the formation of significant quantities of the copper-rich phase ($CuZn_4$ precipitate) in the interdendritic region, while the addition of extra magnesium promoted the formation of the magnesium-rich phase and changed not only the morphology of the primary dendrites but also its relative content. Besides, an increase in the relative primary eutectic structure and a decrease in the quantity of the lamellae eutectoid structure were observed. Additionally, the secondary lamellar eutectic became more refined in the presence of higher magnesium content. All the cooling curves are in agreement with the observed microstructure. Both elements, copper and magnesium, also promoted an increase in the hardness of the Zn–4Al hypoeutectic alloys due to the formation of $CuZn_4$ phase and to the secondary lamellae eutectic refinement, respectively.

1. Introduction

It is well known that the study of microstructure formation during the solidification process is of fundamental importance to understand and to optimize the properties of materials. Zn–Al alloys form a variety of commercial alloys with vast and diverse properties and applications. Therefore, most of the research in this field has recently been concentrated on the Zn–Al hypereutectic alloys (ZA family with Al contents higher than 5.1 wt.% Al) developed in the middle of the 1970s and on Zn–Al eutectoid and monotectoid alloys [1–11]. These Zn–Al alloys have been modified by the addition of many elements in order to improve the mechanical and tribological properties and corrosion resistance. The elements most often added are copper [2,3], magnesium [4] and silicon [5,6]. The Zn–Al hypoeutectic alloys (with Al contents smaller than 5.1 wt.% Al) are the earliest Zn–Al alloys that have been largely used in many engineering applications nowadays and consequently there is interest in studies on the influence of chemical composition in this microstructure, which may improve the properties of these alloys.

According to the Zn–Al binary phase diagram (Fig. 1) there are three important invariant phase transformations that can take place in the Zn–Al alloys: a peritectic transformation at 28.4 wt.% of aluminum and 443 °C, a eutectic transformation at 5.1 wt.% of aluminum and 382 °C and a eutectoid transformation at 22 wt.% of aluminum and 275 °C. When a hypoeutectic alloy solidifies, the following sequence of microstructure formation is observed. The formation of primary dendrites of zinc-rich phase (η-phase) containing 98.86 wt.% of zinc at 382 °C that has a hexagonal close-packed crystalline structure. Below this temperature, a eutectic structure is established from the remaining liquid enriched with a solute segregation, which is formed by the η-phase and a second phase of face-centered cubic crystalline structure named β-phase. The β-phase is constituted of 22 wt.% of aluminum and will be

---

* Corresponding author. Tel.: +55 51 3353 7844; fax: +55 51 3353 4840.
E-mail address: carlos.santos@pucrs.br (C.A. dos Santos).

0925-8388/$ – see front matter © 2009 Elsevier B.V. All rights reserved.
doi:10.1016/j.jallcom.2009.08.125

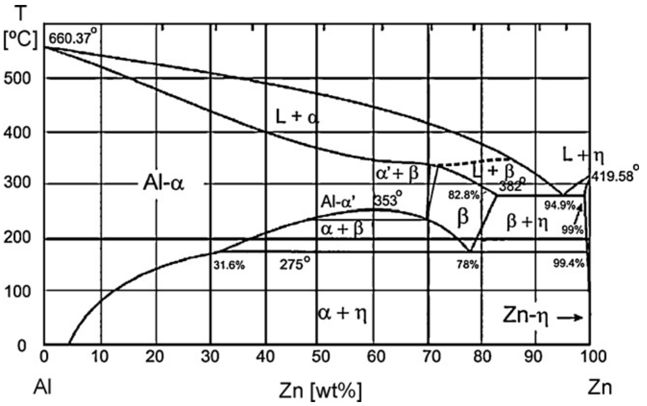

Fig. 1. Binary Al–Zn equilibrium phase diagram [18].

present until 275 °C when a eutectoid transformation occurs generating α + η lamellae structure. During the subsequent cooling, the eutectoid decomposition will affect only the composition of the β-phase inside the lamellae structure, and not the η-phase [1,8,9].

However, the addition of copper and magnesium elements could modify the properties of Zn-alloys since they can change the phase transformation temperatures and the phase relative quantity and compositions, as well as promote the new phase precipitation (Fig. 2). It has also been reported that both copper and magnesium decrease the eutectic temperature. Besides, small amounts of copper and magnesium are necessary to achieve the best combination of mechanical properties and castability [1].

Copper has low solubility in zinc, which leads to a concentration of the copper solute content in the eutectic liquid during the final stage of solidification and as a consequence a metastable ε-precipitate ($CuZn_4$ intermetallic compound) can appear when a copper amount exceeds 1 wt.% [2,3]. For a lower concentration (<1 wt.%) copper is distributed almost uniformly in a macro and microscopic scale, presenting complete solubility in the zinc matrix. At a higher concentration (>1 wt.%) copper is found in dissolution as well as in the form of precipitates, mainly as an intermetallic compound $CuZn_4$. According to Auras and Schvezov [8] copper is present in a ε-precipitate which decomposes with time and produces the dimensional instability. For low copper concentrations the reaction does not take place and the alloy is stable. Zhu et al. [9,10] observed, for a eutectoid Zn–Al based alloy, that the presence of copper allows the formation of the intermetallic compound, $CuZn_4$ (ε-phase) at the eutectic temperature (377 °C) through a ternary eutectic reaction ($L \rightarrow \alpha + \eta + \varepsilon$). At a lower temperature of 268 °C, a ternary stable phase known as Al_4Cu_3Zn (T′-phase) will result from the reaction of ($\alpha + \varepsilon \rightarrow \eta + T'$). The formation of copper-rich intermetallic compound precipitate produces a decrease of copper content in the matrix, reducing the solid solution strengthening effect. In addition, the copper-rich particles are harder and more brittle than the matrix increasing the hardness of the alloy, therefore increasing the cracking tendency [2]. Also, these alloy elements form intermetallic compounds mainly with the presence of impurities such as iron, chromium, nickel and silicon present in very small content.

Chen et al. [4] reported that magnesium concentrated preferentially in the primary dendrites in the Zn–Al hypereutectic alloy (ZA 27) and that the addition of this element increases the liquid fraction, leading to an increase of the distance between dendrites, and consequently to a decrease of the hardness.

As cited before, research on the influence of the chemical composition in the microstructure is concentrated on the Zn–Al hypereutectic alloys (ZA family) and Zn–Al eutectoid and monotectoid alloys [1–11], but not on the Zn–Al hypoeutectic alloys, especially when the association of microstructure formation with thermal analysis is considered. Thus, this study investigates the influence of copper and magnesium in temperature transformations during the solidification of Zn–Al hypoeutectic alloys and the resulting microstructure formation is discussed based on Computer-Aided Cooling Curve Analysis (CA-CCA), metallographic and microanalysis. In addition, the hardness of Zn–Al hypoeutectic alloys containing different quantities of copper and magnesium is also investigated.

2. Computer-Aided Cooling Curve Analysis (CA-CCA)

The Computer-Aided Cooling Curve Analysis (CA-CCA) is a low cost method for thermal analysis that can be used in foundries and laboratories, enabling the quantification of the microconstituents present in the casting, the solidification kinetics and the latent heat released during the solidification process. In this technique the melt is thermally monitored during solidification with a thermocouple and an acquisition data system coupled to a numerical method in a computer. The result is a temperature–time cooling curve from liquid metal temperature to ambient temperature. During solidification and consequently liquid–solid and solid–solid phase transformations, the latent heat released by the solidifying phases causes changes in the cooling curve and its derivatives, which are linked to the development of the microstructure and temperatures observed in the as-cast product. The shape of the cooling curve reflects the solidification process of melt under a given solidification condition.

The heat evolution or heat absorption due to the phase transformation is determined by taking the difference between the cooling curve observed in the sample and in a neutral reference (zero curve or baseline curve). In order to generate the zero curve, that portion of the cooling curve not affected by phase transformations is used, where only heat transfer by conduction in the metal is assumed. The amount of heat evolved or absorbed during the phase transformation can be determined by the area between the first derivative of the cooling curve and the zero curve, which can be evaluated using numerical methods of integration [12–16].

The CA-CCA method based on the Newton Thermal Analysis Method utilizes the Fourier's heat transfer equilibrium equation. The energy balance applied to the metal–mold system considering only heat transfer conduction can be written by the General Equation of Heat Conduction in Unsteady State, in its one-dimensional form, which can be analyzed by:

$$\rho \cdot c_{\text{p}} \cdot \frac{\partial T}{\partial t} = k \cdot \frac{\partial^2 T}{\partial x^2} + \dot{q} \tag{1}$$

where ρ, c_{p}, k are respectively density [kg m^{-3}], specific heat [J kg^{-1} K^{-1}] and thermal conductivity [W m^{-1} K^{-1}], $\partial T/\partial t$ is cooling rate [k s^{-1}],, T is temperature [K], t is time [s] and x is distance along the x-axis [m]. The term $\dot{q}$ in Eq. (1) represents the term associated to internal heat generation due to the phase change, and is given by:

$$\dot{q} = \rho \cdot L \cdot \frac{\partial f_{\text{S}}}{\partial t} \tag{2}$$

where L is the latent heat of fusion [J kg^{-1}] and f_{S} is the solid fraction during phase change along the solidification range (liquidus and solidus temperatures). Eq. (2) can be related to temperature as follows:

$$\frac{\partial f_{\text{S}}}{\partial t} = \frac{\partial f_{\text{S}}}{\partial T} \cdot \frac{\partial T}{\partial t} \tag{3}$$

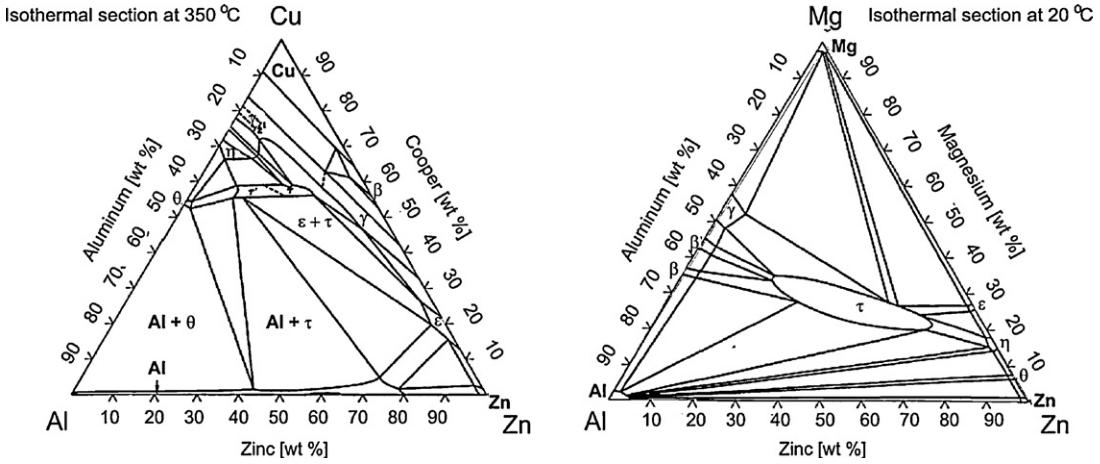

Fig. 2. Ternary Al–Zn–Cu (a) and Al–Zn–Mg (b) equilibrium phase diagrams [18].

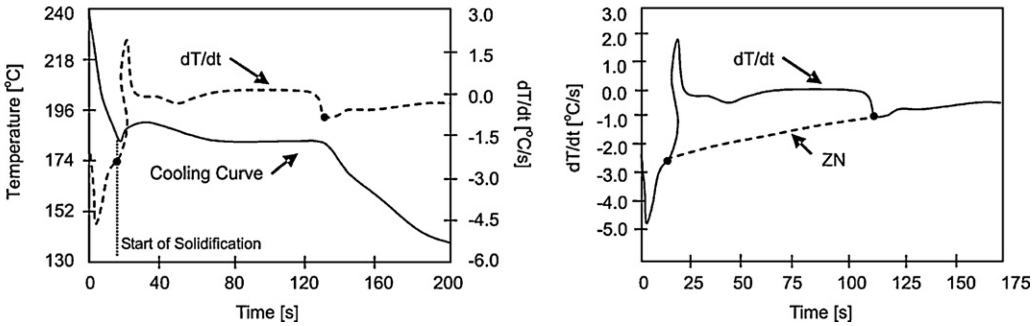

Fig. 3. Representation of the CA-CCA method used [13].

and substituting Eq. (3) in Eq. (2) and then in Eq. (1), yields:

$$\underbrace{\rho \cdot c_\mathrm{p} \cdot \frac{\partial T}{\partial t}}_{Q_\mathrm{A}} = \underbrace{k \cdot \frac{\partial^2 T}{\partial x^2}}_{Q_\mathrm{C}} + \underbrace{\rho \cdot L \cdot \left(\frac{\partial f_\mathrm{S}}{\partial T} \cdot \frac{\partial T}{\partial t}\right)}_{Q_\mathrm{S}} \tag{4}$$

where Q_A is the variation of the temperature of the element in function of the time, Q_C is the instantaneous heat flow transferred by conduction from the considered element to the next element and Q_S is the heat formation in the element due to the solidification latent heat. Then:

$$Q_\mathrm{S} = Q_\mathrm{A} - Q_\mathrm{C} \tag{5}$$

or:

$$Q_\mathrm{S} = \rho \cdot c_\mathrm{p} \frac{\partial T}{\partial t} - k \cdot \frac{\partial^2 T}{\partial x^2} \tag{6}$$

resulting in:

$$Q_\mathrm{S} = \rho \cdot c_\mathrm{p} \cdot \frac{\partial T}{\partial t} - \mathrm{ZN} \tag{7}$$

where ZN indicates the cooling rate evolution that the system would show if the latent heat released from the solidification of the real system were not present.

Before the time of start and after the time of end of solidification, $Q_\mathrm{S} = 0$ and Eq. (7) shows that there is a ZN for the liquid of the melt and for the solid state, numerically equal to the corresponding $\mathrm{d}T/\mathrm{d}t$ evolution immediately before and after solidification. In this study the ZN is calculated using the first derivative values corresponding with times of start and end of solidification, as can be observed in Fig. 3.

3. Experimental procedure

In order to study the influence of copper and magnesium addition on Zn–Al hypoeutectic alloys, ternary and quaternary alloys were prepared with different amounts of copper and magnesium (weight percent). Table 1 shows the chemical composition of five different Zn–Al–Cu–Mg alloys being studied. The alloy identified as Zn–4Al–3Cu–0.5Mg commercial alloy was acquired in the national market and is already a modified version of the Zn–Al hypoeutectic alloy known as No. 2 alloy (Zamac 2—standard), whose chemical composition was also included in Table 1 only for comparison purposes. It can be observed that the commercial alloy being considered already has one upgrade in the copper and magnesium amount in relation to the Zamac 2—standard alloy. Two ternary alloys (Zn–4Al–3Cu and

Table 1
Chemical composition of Zn–Al hypoeutectic alloys.

Alloy	Element (wt.%)			
	Al	Cu	Mg	Zn
No. 2 alloy (Zamac 2—standard) [17]	3.50–4.50	2.50–3.00	0.02–0.05	Balance
Zn–4Al–3Cu ternary alloy	3.80	2.90	–	Balance
Zn–4Al–1Mg ternary alloy	3.80	–	0.96	Balance
Zn–4Al–3Cu–0.5Mg commercial alloy	3.80	2.90	0.46	Balance
Zn–4Al–4Cu–0.5Mg quaternary alloy	3.80	3.90	0.46	Balance
Zn–4Al–3Cu–1Mg quaternary alloy	3.80	2.90	0.96	Balance

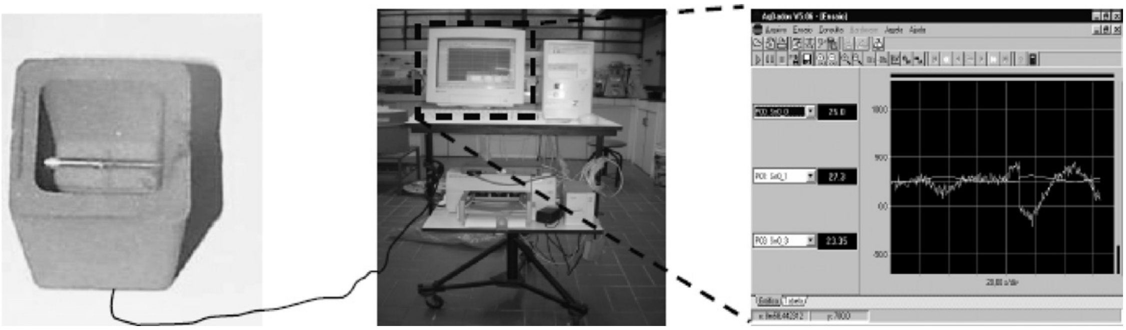

Fig. 4. Schematic representation of the system utilized in the thermal analyses.

Zn–4Al–1Mg) were also obtained in order to better understand the behavior of these elements with regards to temperature transformations. The chemical compositions of all alloys studied, presented in Table 1, were determined by optical emission spectrometry and they correspond to average values of five measurements in each sample. The approximate amounts of residual impurities were 0.25 wt.% for all alloys.

The experimental ternary alloys were obtained by adding aluminum, copper or magnesium in the elementary form directly into the melted zinc. The modified quaternary alloys were obtained by adding copper or magnesium directly into the melt of the commercial alloy. The alloys were melted in graphite crucibles using a resistive furnace and after that they were poured into a special rectangular sand mold (25 mm × 25 mm × 75 mm). A ceramic encapsulated K-type thermocouple, located in the center of the mold cavity, was used to obtain the cooling curves during solidification process. The system was previously calibrated using commercially pure aluminum. In all experiments the pouring temperature was approximately 100 °C above the liquidus temperature and the average solidification time was approxi-

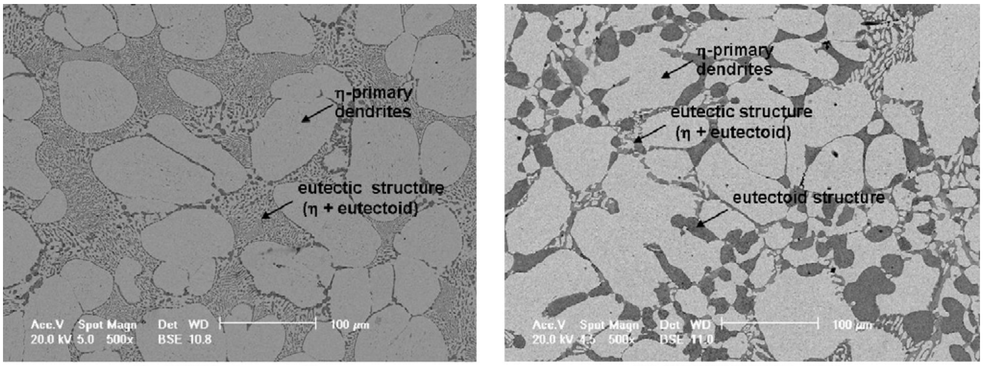

Zn-4Al-3Cu ternary alloy

Zn-4Al-1Mg ternary alloy

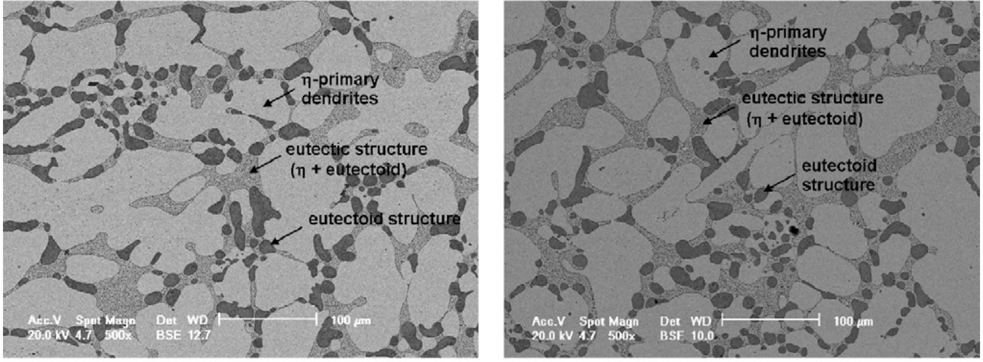

Zn-4Al-3Cu-0.5Mg commercial quaternary alloy

Zn-4Al-4Cu-0,5Mg modified quaternary alloy

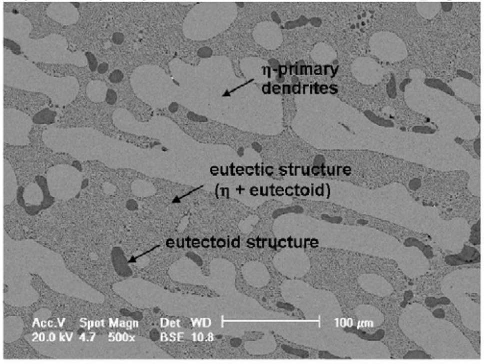

Zn-4Al-3Cu-1Mg modified quaternary alloy

Fig. 5. Microstructures of the Zn–Al hypoeutectic alloys.

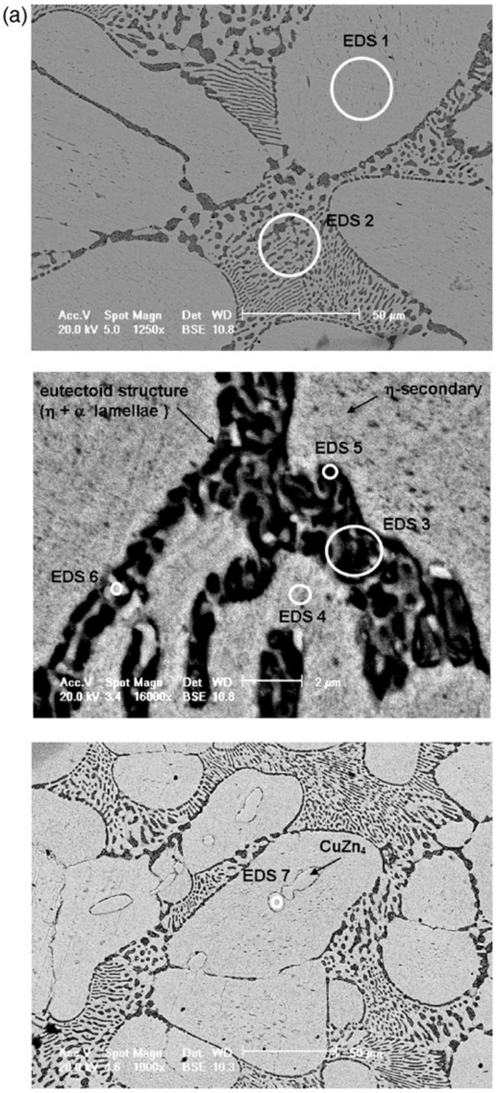

(b)

EDS 1 – Matrix (η-Zn rich dendrites)

Elem	Wt %
AlK	4.06
CuK	3.73
ZnK	92.21
Total	100.00

EDS 2 – Eutectic interdendrictic structure (η-phase + eutectoid)

Elem	Wt %
AlK	12.79
CuK	3.52
ZnK	83.70
Total	100.00

EDS 3 – Eutectoid structure (from eutectic: η + α)

Elem	Wt %
AlK	29.19
CuK	2.74
ZnK	68.07
Total	100.00

EDS 4 – Eutectic (η-phase)

Elem	Wt %
AlK	1.41
CuK	4.57
ZnK	94.01
Total	100.00

EDS 5 – Eutectoid (black lamellae)

Elem	Wt %
AlK	39.08
ZnK	60.92
Total	100.00

EDS 6 – Eutectoid (white lamellae)

Elem	Wt %
AlK	14.67
CuK	7.05
ZnK	78.28
Total	100.00

EDS 7 – $CuZn_4$ (ε-phase)

Elem	Wt %
CuK	17.41
ZnK	82.59
Total	100.00

Fig. 6. SEM images showing the typical microstructure of the Zn–4Al–3Cu ternary alloy. (a) Microstructures; (b) EDS.

mately 650 s. Fig. 4 presents a schematic representation of the thermal analyses system.

The chemical compositions of the phases and precipitates were achieved by EDS (Energy Dispersive X-Ray Spectroscopy) in a SEM (Scanning Electron Microscopy). The typical phase transformation temperatures were determined by means of the CA-CCA method (Computer-Aided Cooling Curve Analysis) making use of one acquisition data system and a software developed for this purpose. Traditional metallographic techniques were used for microstructure characterization of the alloys in the SEM, using 5% Nital etch for 30 s. Besides, the Brinell hardness of the alloys was measured with the purpose of obtaining information about their mechanical properties.

4. Results and discussion

4.1. Microstructure of Zn–Al hypoeutectic alloys

Fig. 5 shows the typical overviews of the microstructures for ternary and quaternary alloys as well as for the commercial alloy. Figs. 3–7 present details of microstructure of all alloys studied showing the precipitated phases and their respective chemical compositions, as determined by EDS.

According to Fig. 5, the microstructure of all alloys is basically composed by a dendrite matrix corresponding to a primary zinc-rich phase (η-phase), one eutectic interdendritic microconstituent and one eutectoid isolated region, with the exception of the Zn–4Al–3Cu ternary alloy. The fact that the eutectoid structure (η + α lamellae) was not observed in Zn–4Al–3Cu ternary alloy can be an indicative that the magnesium is responsible for the formation of this isolated eutectoid microconstituent. On the other hand, by comparing Fig. 5a (Zn–4Al–3Cu alloy) and Fig. 5b (Zn–4Al–1Mg alloy), copper has a high tendency to form the eutectic interdendritic structure. Thus, in the quaternary alloys, where both elements are present, the relative quantity of the microconstituents is influenced by the percentages of copper and magnesium contents added to the alloy. Comparing Fig. 5c and d, which correspond to Zn–4Al–3Cu–0.5Mg and Zn–4Al–4Cu–0.5Mg respectively, it is possible to observe an increment in the relative quantity of the eutectic structure in the Zn–4Al–4Cu–0.5Mg alloy (Fig. 5d) and a decrease in the relative quantity of the primary dendrite phase in relation to the first one because of the higher copper content in this alloy. The effects of simultaneous addition of copper and magnesium are particularly evident in the quaternary alloy with higher magne-

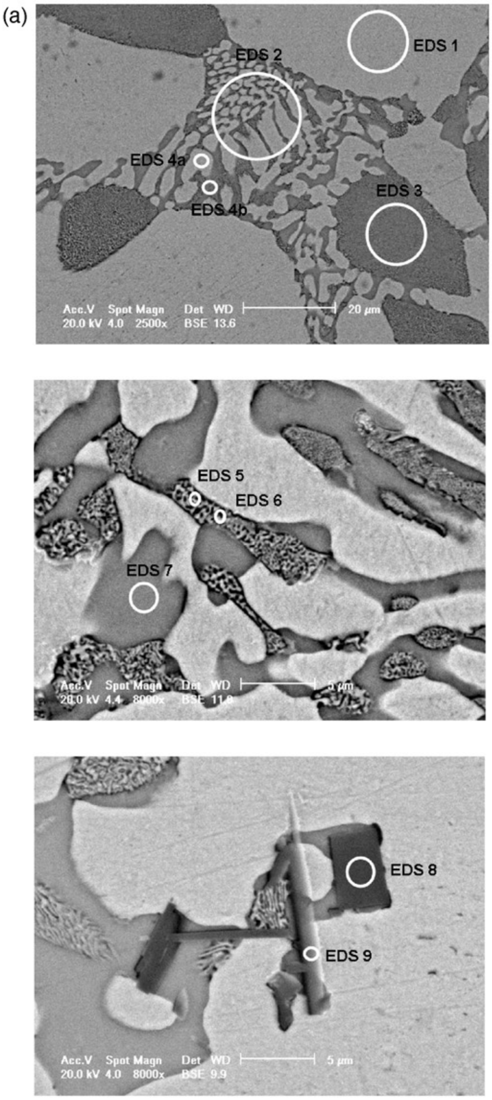

(b)

EDS 1 – Matrix (η-phase)

Elem	Wt %
AlK	2.50
ZnK	97.50
Total	100.00

EDS 2 – Eutectic structure (η-phase + eutectoid)

Elem	Wt %
AlK	7.49
MgK	3.70
ZnK	88.82
Total	100.00

EDS 3 – Eutectoid structure (isolated η + α)

Elem	Wt %
AlK	23.76
ZnK	76.24
Total	100.00

EDS 4 – Eutectic: a (η-phase); b (eutectoid)

Elem	Wt %
AlK	2.51
ZnK	97.49
Total	100.00

Elem	Wt %
AlK	22.62
MgK	1.58
ZnK	75.80
Total	100.00

EDS 5 – Eutectoid (black lamellae)

Elem	Wt %
AlK	14.45
MgK	7.90
ZnK	77.66
Total	100.00

EDS 6 – Eutectoid (white lamellae)

Elem	Wt %
AlK	1.91
ZnK	98.09
Total	100.00

EDS 7 – Mg-rich phase

Elem	Wt %
AlK	1.32
MgK	14.67
ZnK	84.01
Total	100.00

EDS 8 **Impurities** **EDS 9**

Elem	Wt %
AlK	51.52
SiK	3.09
MnK	1.51
FeK	32.13
ZnK	11.74
Total	100.00

Elem	Wt %
AlK	35.36
SiK	1.51
MnK	1.57
FeK	11.03
ZnK	50.53
Total	100.00

Fig. 7. SEM images showing the typical microstructure of the Zn–4Al–1Mg ternary alloy. (a) Microstructures; (b) EDS.

sium content (Zn–4Al–3Cu–1Mg, Fig. 5e), where it is possible to observe a considerable difference between the relative quantities of the microconstituents in relation to other quaternary alloys. In this alloy there was a significant increase of eutectic interdendritic in detriment of both primary dendrites and isolated eutectoid. The increment in the proportion of eutectic interdendritic structure contributes to Mg-rich phase (Fig. 10—EDS 4) formation in this region, probably due to a magnesium segregation phenomenon. The Mg-rich phase is present in all alloys containing magnesium and its quantity increases with magnesium amount added. Additionally, the presence of high magnesium content changed the morphology of the primary dendrites.

Table 2
Solidification interval of Zn–Al hypoeutectic alloys determined from cooling curves.

Alloy	Temperature corresponding to the solidification interval
No. 2 alloy (Zamac 2—standard) [17]	390–379 °C ($\Delta T = 11$ °C)
Zn–4Al–3Cu ternary alloy	396–369 °C ($\Delta T = 27$ °C)
Zn–4Al–1Mg ternary alloy	371–322 °C ($\Delta T = 49$ °C)
Zn–4Al–3Cu–0.5Mg commercial alloy	388–339 °C ($\Delta T = 49$ °C)
Zn–4Al–4Cu–0.5Mg quaternary modified alloy	387–348 °C ($\Delta T = 39$ °C)
Zn–4Al–3Cu–1Mg quaternary modified alloy	377–335 °C ($\Delta T = 42$ °C)

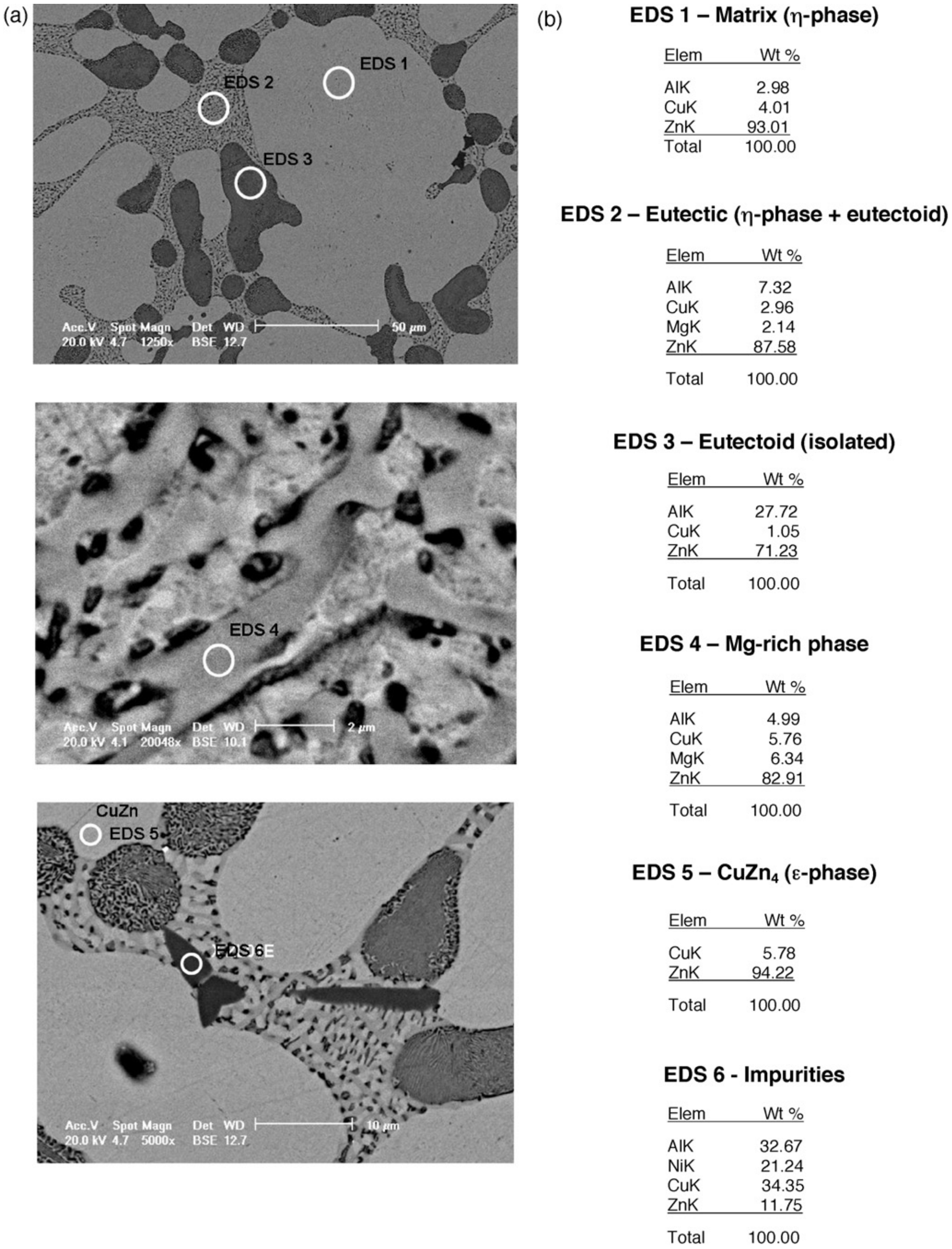

EDS 1 – Matrix (η-phase)

Elem	Wt %
AlK	2.98
CuK	4.01
ZnK	93.01
Total	100.00

EDS 2 – Eutectic (η-phase + eutectoid)

Elem	Wt %
AlK	7.32
CuK	2.96
MgK	2.14
ZnK	87.58
Total	100.00

EDS 3 – Eutectoid (isolated)

Elem	Wt %
AlK	27.72
CuK	1.05
ZnK	71.23
Total	100.00

EDS 4 – Mg-rich phase

Elem	Wt %
AlK	4.99
CuK	5.76
MgK	6.34
ZnK	82.91
Total	100.00

EDS 5 – $CuZn_4$ (ε-phase)

Elem	Wt %
CuK	5.78
ZnK	94.22
Total	100.00

EDS 6 - Impurities

Elem	Wt %
AlK	32.67
NiK	21.24
CuK	34.35
ZnK	11.75
Total	100.00

Fig. 8. SEM images showing the typical microstructure of the Zn–4Al–3Cu–0.5Mg commercial alloy. (a) Microstructures; (b) EDS.

Fig. 6 presents details of both matrix and interdendritic structures for Zn–4Al–3Cu ternary. The matrix is a η-zinc rich phase—EDS 1 containing copper and aluminum, the eutectic interdendritic structure is constituted of η-phase and a eutectoid structure—EDS 2, which is composed by lamellas of η- and α-phases—EDS 3. The EDS 4 shows the chemical composition of the η-phase located into the eutectic structure and the EDS 5 shows the chemical composition of the black lamellae of eutectoid phase, while the EDS 6 corresponds to the white lamellae of eutectoid phase. The eutectoid phases ($\eta+\alpha$) are probably associated to

Table 3
Temperatures corresponding to each phase formation on Zn–Al hypoeutectic alloys determined from cooling curves.

Alloy	Formation of Zn-rich solid solution (η-Zn rich dendrites)	Formation of metastable ε-phase ($CuZn_4$)	Formation of Zn, Al and Cu primary eutectic	Formation of Zn, Al, Cu and Mg secondary eutectic
Zn–4Al–3Cu ternary alloy	396 °C	387 °C	379 °C	Non observed
Zn–4Al–1Mg ternary alloy	371 °C	Non observed	356 °C	322 °C
Zn–4Al–3Cu–0.5Mg commercial alloy	388 °C	374 °C	369 °C	339 °C
Zn–4Al–4Cu–0.5Mg quaternary modified alloy	387 °C	375 °C	368 °C	348 °C
Zn–4Al–3Cu–1Mg quaternary modified alloy	377 °C	Non observed	350 °C	335 °C

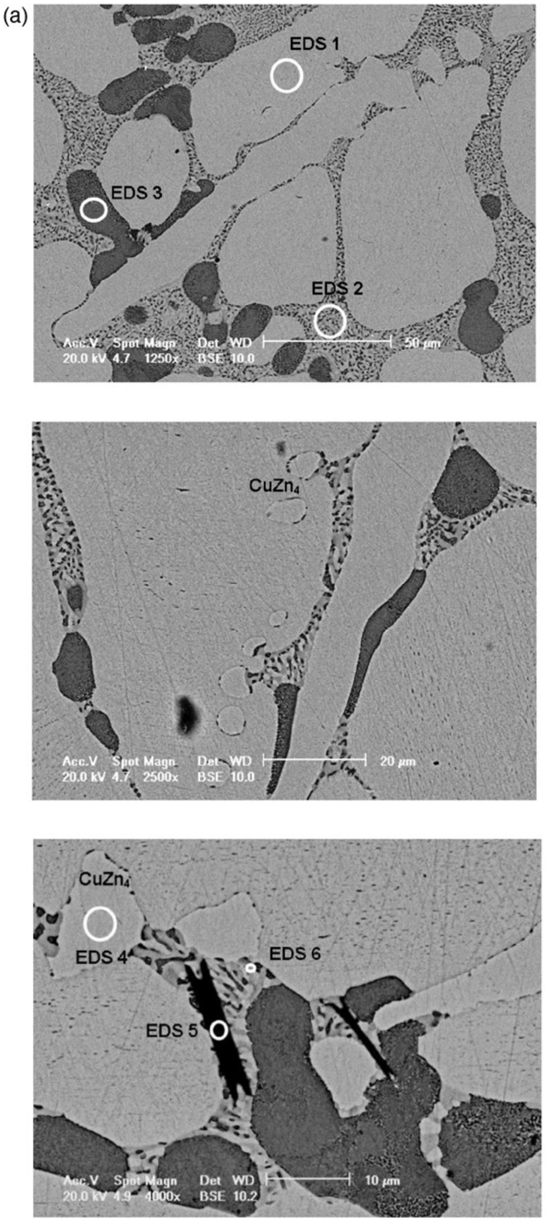

(b)

EDS 1 – Matrix (η-phase)

Elem	Wt %
AlK	2.98
CuK	4.01
ZnK	93.01
Total	100.00

EDS 2 – Eutectic (η-phase + eutectoid)

Elem	Wt %
AlK	8.58
CuK	4.17
MgK	2.09
ZnK	85.16
Total	100.00

EDS 3 – Eutectoid (isolated)

Elem	Wt %
AlK	26.36
CuK	2.25
ZnK	71.39
Total	100.00

EDS 4 – $CuZn_4$ (ε-phase)

Elem	Wt %
CuK	15.67
ZnK	84.33
Total	100.00

EDS 5 - Impurities

Elem	Wt %
AlK	49.72
SiK	1.29
FeK	29.93
ZnK	19.06
Total	100.00

EDS 6 – Mg-rich phase

Elem	Wt %
AlK	2.50
CuK	4.46
MgK	4.97
ZnK	88.07
Total	100.00

Fig. 9. SEM images showing the typical microstructure of the Zn–4Al–4Cu–0.5Mg modified alloy. (a) Microstructures; (b) EDS.

a transformation from the β-phase according to phase diagram (Fig. 1). The copper addition promoted a formation of copper-rich particles (EDS 7), probably associated to the formation of ε-phase ($CuZn_4$) according to results published by Savaskan et al. [3] and Zhu et al. [4,9].

In Fig. 7, which details the microstructure for Zn–4Al–1Mg ternary, it can be observed that the matrix is a η-zinc rich phase—EDS 1 containing only zinc and aluminum, the eutectic interdendritic containing zinc, magnesium and aluminum—EDS 2, lamellas of η- and α-phases—EDS 3 have the presence of zinc and aluminum only. The magnesium addition promoted a formation of magnesium-rich phase (EDS 7) only in the interdendritic phase between the η-phase and eutectoid phase.

The eutectic interdendritic structure in all quaternary alloys (Figs. 8–10) contains zinc, aluminum, copper and magnesium (primary eutectic—EDS 2) and the eutectoid structure (isolated EDS 3) has the presence of zinc, aluminum and copper, in addition to a magnesium-rich phase. The commercial alloy (Zn–4Al–3Cu–0.5Mg) considered the reference alloy presents a microstructure with a high quantity of the primary dendrites, a small quantity of the interdendritic microconstituent and some isolated eutectoid structure (Fig. 8). In the quaternary alloy with extra copper content (Zn–4Al–4Cu–0.5Mg) it was possible to observe in the microstructure (Fig. 9) a more significant quantity of copper-rich phase when compared to the others alloys. This observation is in accordance with literature [2,3,9] which found that the addition of copper above 1 wt.% results in the formation of copper-rich ε-phase ($CuZn_4$) and that the number, size and distribution of the ε-phase particles increase with the copper content.

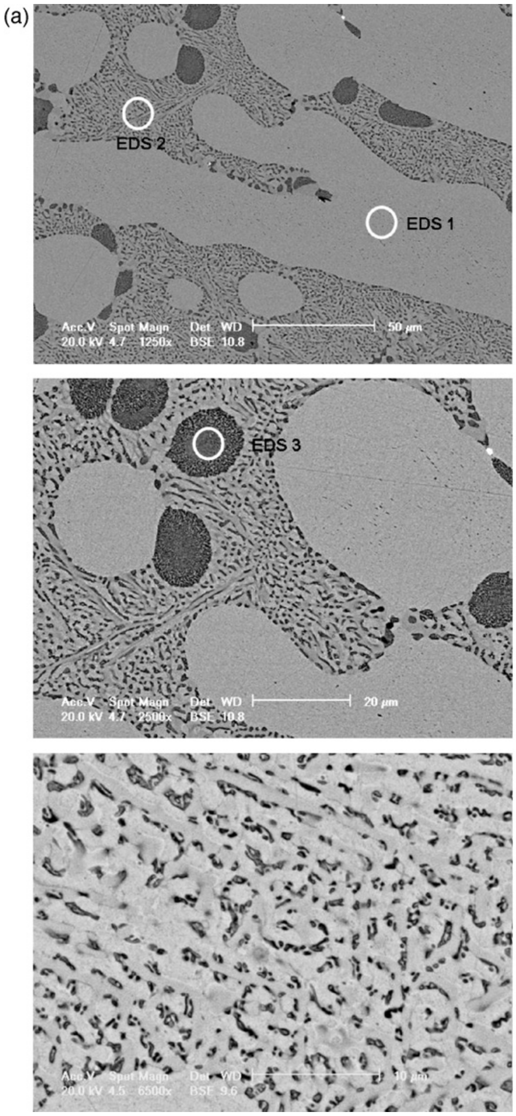

(b)

EDS 1 – Matrix (η-phase)

Elem	Wt %
AlK	1.99
CuK	3.72
ZnK	94.29
Total	100.00

EDS 2 – Eutectic (η-phase + eutectoid)

Elem	Wt %
AlK	9.35
CuK	3.23
MgK	2.29
ZnK	85.13
Total	100.00

EDS 3 – Eutectoid (isolated)

Elem	Wt %
AlK	28.06
CuK	1.76
ZnK	70.17
Total	100.00

EDS 4 – Mg-rich phase

Elem	Wt %
AlK	2.57
CuK	5.94
MgK	5.95
ZnK	85.54
Total	100.00

Fig. 10. SEM images showing the typical microstructure of the Zn–4Al–3Cu–1Mg modified alloy. (a) Microstructures; (b) EDS.

However, with the addition of extra magnesium in the quaternary alloy (Zn–4Al–4Cu–1.0Mg), Fig. 10, besides the alteration in the morphology of the primary dendrites and in the relative content of the microconstituents, the lamellae eutectoid became more refined. It can also be seen that the quantity of Mg-rich phase increased in this region when compared to other alloys. This result agrees with the work of Chen et al., who studied the effects of magnesium and rare earth additions on the semi-solid microstructure of a zinc alloy ZA 27 [4]. In this alloy the presence of $CuZn_4$ intermetallic compound on the microstructure was not observed.

Furthermore, different types of precipitated phases containing aluminum, iron, chromium, manganese and nickel elements could be found in all alloys, either ternary or quaternary alloys, as can be seen in Fig. 7—EDS 8 and EDS 9, Fig. 8—EDS 6 and Fig. 9—EDS 5. These kinds of precipitates are associated with the presence of impurities.

4.2. Cooling curves of the Zn–Al hypoeutectic alloys

Fig. 11 shows the typical cooling curves of the Zn–4Al–3Cu and Zn–4Al–1Mg ternary alloys, Zn–4Al–3Cu–0.5Mg commercial alloy, and Zn–4Al–4Cu–0.5Mg and Zn–4Al–4Cu–0.5Mg quaternary modified alloys, respectively, as well as the first derivatives of the cooling curves.

The temperatures corresponding to solidification interval for all alloys are shown in Table 2. All alloys, ternary and quaternary, containing a high copper and magnesium amount exhibited a larger solid–liquid temperature range compared to the No. 2 standard alloy, indicating that the presence of copper and magnesium can promote the formation of new phases at lower temperatures, as can be observed in the different deflection of the cooling curves during the solidification interval. However, there is no significant modification on the liquidus temperature in relation to standard alloy, except for alloys containing 1 wt.% of magnesium, in both cases ternary and quaternary alloys, which exhibited lower values than other alloys.

In the cooling curves of the ternary alloys (Fig. 11a and b) the formation of three phases during the solidification interval can be observed. The cooling curves of Zn–4Al–3Cu–0.5Mg commercial alloy and Zn–4Al–4Cu–0.5Mg modified alloy clearly display the presence of four phase formation, according to Fig. 11c and d. This is in agreement with the microstructure, where four main different structures can be differentiated. However, the cooling curve of Zn–4Al–3Cu–1Mg alloy (Fig. 11e) presents only three phase formation, suppressing the appearance of the $CuZn_4$ intermetallic

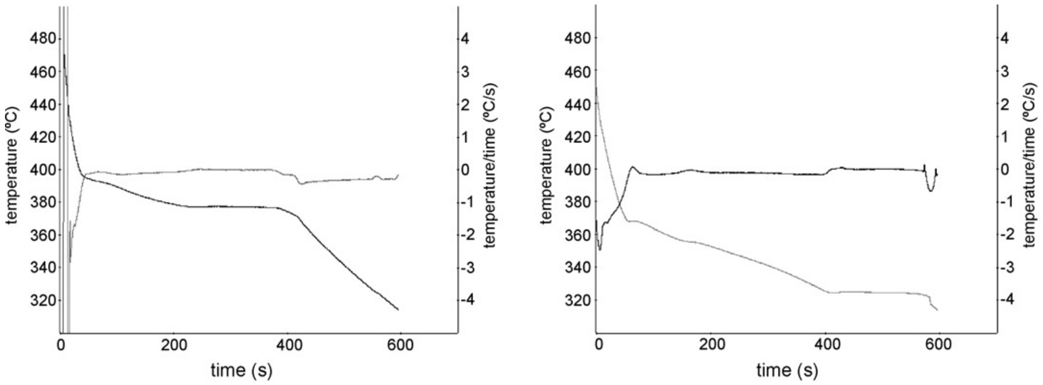

(a) Zn-4Al-3Cu ternary alloy (b) Zn-4Al-1Mg ternary alloy

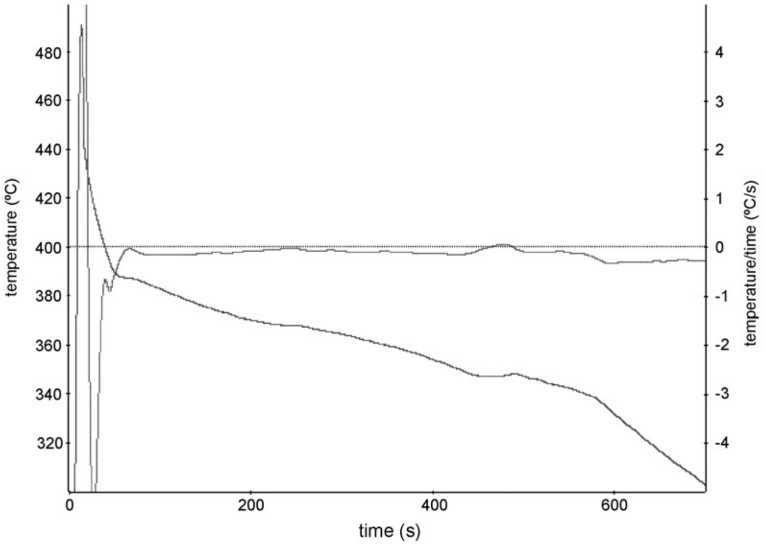

(c)Zn-4Al-3Cu-0.5Mg commercial alloy

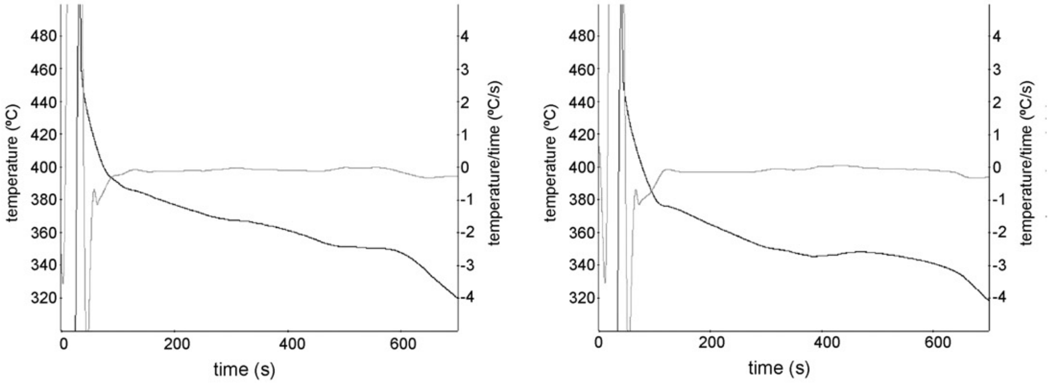

(d) Zn-4Al-4Cu-0.5Mg modified alloy (e) Zn-4Al-3Cu-1Mg modified alloy

Fig. 11. Cooling and the first derivative curves for Zn–4Al hypoeutectic alloys.

compound. The temperatures corresponding to all phases formation extracted from cooling curves are summarized in Table 3.

In addition, it can be observed that the time dispended on the formation of each phase depends on the amount of both copper and magnesium in the alloy, and as a consequence this fact will promote a variation between relative quantities of the phase present in the material, modifying its properties. This is particularly evident in the case of alloy with high magnesium amount (Zn–4Al–4Cu–1Mg) whose last transformation corresponding to formation of a secondary eutectic takes much more time. Such fact is in agreement with the microstructure of this alloy, where an increase in the quantity of the secondary lamellar eutectic structure and a decrease in the quantity of the primary particles and isolated eutectoid structure can be observed.

4.3. Hardness of the Zn–Al hypoeutectic alloys

The hardness of the ternary and quaternary alloys increased with the content of copper and magnesium, e.g., the No. 2 alloy is the alloy that presented the lowest hardness value when com-

Table 4
Brinell hardness of Zn–4Al hypoeutectic alloys.

Zn–4Al hypoeutectic alloy	Brinell hardness ($D = 5$ mm)
No. 2 alloy (Zamac 2—standard) [17]	100 HB
Zn–4Al–3Cu ternary alloy	107 HB
Zn–4Al–1Mg ternary alloy	97 HB
Zn–4Al–3Cu–0.5Mg commercial alloy	112 HB
Zn–4Al–4Cu–0.5Mg quaternary modified alloy	131 HB
Zn–4Al–3Cu–1Mg quaternary modified alloy	133 HB

pared to the others, as can be seen in Table 4. In the case of Cu-rich alloys, the improvement obtained in the hardness can be explained in terms of the superior relative content of $CuZn_4$ phase present in the microstructure, which is in accordance with literature [2,3]. The Mg-rich quaternary alloy (Zn–4Al–3Cu–1Mg) exhibited the highest value of hardness and this fact can be associated to the microstructure refinement, especially in the case of lamellae eutectoid (Fig. 7).

5. Conclusions

The presence and the amount of copper and magnesium have a significant influence on the properties of the Zn–4Al hypoeutectic alloys since distinct microstructures can be formed during solidification. This indicates that a precise chemical composition control during the industrial production is necessary so as to prevent defects formation such as dimensional instability, hot cracking and poor mechanical properties. Additionally, according to the cooling curves obtained, the presence of these elements leads to modifications in the temperatures, in the kinetic and in the chemical compositions of phases formed.

For the ternary alloys, it can be concluded that the copper content suppresses the isolated eutectoid structure, while the magnesium content makes this formation easier. The ternary alloys presented hardness values lower than those from quaternary alloys, but higher than No. 2 alloy.

The addition of extra copper promoted:

- A formation of a significant quantity of the copper-rich phase ($CuZn_4$ precipitate) in the interdendritic region, which is probably responsible for the increase in the hardness;
- An increase in the hardness of about 17% when compared to the commercial alloy;
- A decrease of about 25% in the solidification interval when compared to the commercial alloy.

The addition of extra magnesium promoted:

- An alteration in the morphology of the primary particles decreasing its relative content in the alloy;
- An increase in the relative primary eutectic structure;
- A decrease in the quantity of the lamellar eutectoid structure;
- A suppression of $CuZn_4$ intermetallic compound formation;
- A refinement of the secondary lamellae eutectic that could lead to the observed increase in the hardness of the alloy (19% when compared to commercial alloy);
- A formation of a new Mg-rich phase at low temperature, which is probably responsible for the increase in the solid–liquid temperature range.

References

[1] M.T.A. El-Kahir, A. Daoud, A. Ismail, Mater. Lett. 58 (2004) 1754–1760.
[2] T. Savaskan, M.S. Turhal, Mater. Charact. 51 (2003) 259–270.
[3] T. Savaskan, A.P. Hekimoglu, G. Purçek, Tribol. Int. 37 (2004) 45–50.
[4] T.J. Chen, Y. Hao, J. Sun, Y.D. Li, Sci. Technol. Adv. Mater. 4 (2003) 495–502.
[5] B.K. Prasad, Mater. Sci. Eng. A 367 (2003) 63–73.
[6] T. Savaskan, O. Bican, Mater. Sci. Eng. A 404 (2005) 259–269.
[7] S.R. Casolco, J. Negrete-Sanchez, G. Torres-Villasenor, Mater. Charact. 51 (2003) 63–67.
[8] R. Auras, C. Schvezov, Light Metals, Proceedings, TMS, CA, USA, 1999.
[9] Y.H. Zhu, H.C. Man, W.B. Lee, Mater. Sci. Eng. A 268 (1999) 147–153.
[10] Y.H. Zhu, W.B. Lee, S. To, Mater. Res. Bull. 38 (2003) 1851–1858.
[11] Z. Mei, Y.H. Zhu, W.B. Lee, T.M. Yue, G.K.H. Pang, Composites—Part A: Appl. Sci. Manuf. 37/9 (2006) 1345–1350.
[12] J.C. Escobedo, M.A. Ramirez, D.A. Cortes, A. Flores, H. Castillejos, F.A. Acosta, in: Reidar Huglen (Ed.), Light Metals, The Minerals, Metals and Materials Society, 1997.
[13] H. Cruz, C. Gonzalez, A. Juarez, M. Herrera, J. Juarez, J. Mater. Proc. Technol. 178 (2006) 128–134.
[14] X. Chen, H. Geng, Y. Li, Mater. Sci. Eng. A 419 (2006) 283–289.
[15] D. Emadi, L.V. Whiting, S. Nafisi, R. Ghomashchi, J. Therm. Anal. Calorim. 81 (2005) 235–242.
[16] B.A. Dedavid, E.M. Costa, C.R.F. Ferreira, J. Therm. Anal. Calorim. 67 (2002) 473–480.
[17] ASM Handbook. Properties and Selection: Nonferrous Alloys and Special—Purpose Materials, vol. 2, ASM International, USA, 1990.
[18] ASM Handbook. Alloy Phase Diagrams, vol. 3, ASM International, USA, 1992.